Design and optimization of a monolithic GaInP/GaInAs tandem solar cell*

Zhang Han(张汉)[1,†], Chen Nuofu(陈诺夫)[2,3,†], Wang Yu(汪宇)[1], Yin Zhigang(尹志岗)[1], Zhang Xingwang(张兴旺)[1], Shi Huiwei(施辉伟)[1], Wang Yanshuo(王彦硕)[1], and Huang Tianmao(黄添懋)[1]

(1 Key Laboratory of Semiconductor Materials Science, Institute of Semiconductors, Chinese Academy of Sciences, Beijing 100083, China)
(2 School of Renewable Energy Engineering, North China Electric Power University, Beijing 102206, China)
(3 National Laboratory of Microgravity, Institute of Mechanics, Chinese Academy of Sciences, Beijing 100080, China)

Abstract: We have theoretically calculated the photovoltaic conversion efficiency of a monolithic dual-junction GaInP/GaInAs device, which can be experimentally fabricated on a binary GaAs substrate. By optimizing the bandgap combination of the considered structure, an improvement of conversion efficiency has been observed in comparison to the conventional $GaInP_2$/GaAs system. For the suggested bandgap combination 1.83 eV/1.335 eV, our calculation indicates that the attainable efficiency can be enhanced up to 40.45% (300 suns, AM1.5d) for the optimal structure parameter (1550 nm GaInP top and 5500 nm GaInAs bottom), showing promising application prospects due to its acceptable lattice-mismatch (0.43%) to the GaAs substrate.

Key words: III–V semiconductor; photovoltaic; tandem solar cell; theoretical efficiency
DOI: 10.1088/1674-4926/31/8/084009 **PACC:** 4280Y; 7865K; 7360L

1. Introduction

III–V semiconductor (SC) tandem photovoltaic (PV) cells in concentrator systems have been widely demonstrated in recent years as an effective pathway to realize higher conversion efficiency, showing promising prospects in both terrestrial and space applications[1−5]. Generally, tandem PV cells are constructed by several series-connected subcells, mainly fabricated by different bandgap III–V SC alloys, through proper tunnel junctions. In this configuration, the apparent drawbacks encountered by the conventional single-junction device, namely large energy loss for the short wavelength and sub-bandgap component of the solar spectrum, have been effectively relaxed by improving the utilization of the spectrum, and enhanced energy conversion is thus expected. For instance, based on a lattice-matched $GaInP_2$/GaAs dual-junction configuration, the available efficiency 32.6% at 1000 suns has also been reported very recently[6]. Moreover, the ongoing enhancement of these encouraging efficiencies is still anticipated by performing more detailed optimization for the operable device structure.

For an elegant electric output of a tandem PV cell, the rigorous current-match relationship between subcells should be satisfied, which in turn requires careful design of the subcell parameters, e.g., a proper combination of bandgap (E_g) and thickness. Consequently, it is necessary for device optimization to incorporate realistic quantum efficiency (QE) relying on these mentioned parameters. Unfortunately, in order to simplify the calculation, previous numerical simulations[7−10] commonly assumed the QE of subcells to be a step-like response to the incident photon, i.e., for the impinging photon with energy higher than the E_g of the material, it will contribute a net electron–hole pair for the photocurrent. Nevertheless, the realistic QE is strongly affected by the absorption of the photons above E_g within a finite subcell thickness and the minority carriers' recombination in different regions of the p–n junction. Evidently, this oversimplified assumption is less meaningful for real device design. To overcome this insufficiency, in this paper we model the PV conversion efficiency (η) for a dual-junction GaInP/GaInAs system by integrating a set of chosen parameters with semiconductor transport equations into the realistic QE parameter and evaluate their potential effects on the electrical performance of the specific device structure.

In this paper, we have modeled the PV conversion efficiency (η) for a dual-junction GaInP/GaInAs system by taking into account the realistic QE parameter. Numerical optimizations have been done by adjusting parameters such as the combination of E_g as well as the specific structure of the cell. Consistent with recent experimental studies[2−4], the possible enhancement of η is expected by developing an acceptable metamorphic system. More importantly, a critical output performance behavior has been clarified by adjusting the thickness of subcells, and feasible structure parameters were also proposed with the aim to achieve higher η than the traditional $GaInP_2$/GaAs tandem cell.

2. Model

In this work our calculations were all performed under AM1.5 direct spectral conditions (ASTM G173-03 Reference Spectra AM1.5d[11]) , at a high concentration of 300 suns and a cell temperature of 300 K. The specific device structure investigated is schematically depicted in Fig. 1, where a monolithic dual-junction GaInP/GaInAs cell is assumed to be fabricated on the GaAs substrate. As an illustrating example, we assumed both subcells have the same emitter thickness (100 nm

* Project supported by the State Key Development Program for Basic Research of China (No. 2010CB933800).
† Corresponding author. Email: hzhang@semi.ac.cn, nfchen@semi.ac.cn
Received 18 November 2009

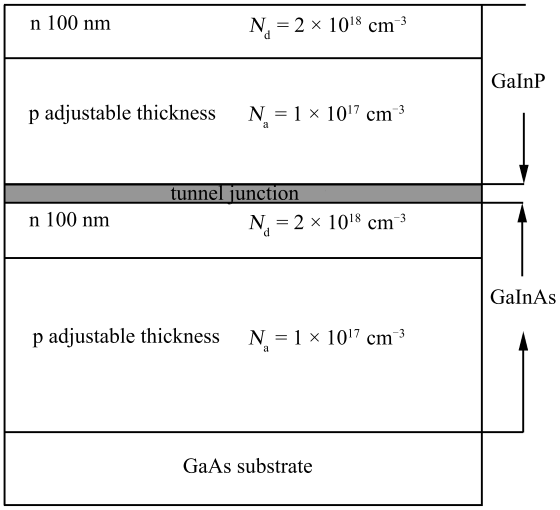

Fig. 1. Schematic diagram of the GaInP/GaInAs dual-junction solar cell.

in our case) and doping profiles, i.e., donor concentration in the emitter $N_d = 2 \times 10^{18}$ cm^{-3} and acceptor concentration in the base $N_a = 1 \times 10^{17}$ cm^{-3}. In contrast to the previous investigations[9, 12], the base thickness of both subcells was assumed to be adjustable in order to perform the structural optimization. By modifying the indium composition, the optimal E_g combination can also be revealed. For convenience in our calculation, several simplifying assumptions were made here, including (1) no series resistance losses and ideal tunnel junction interconnect, and (2) no reflection losses and contact shadowing.

Due to its series-connected characteristic, following the ideal diode equations, the output J–V characteristic of the GaInP/GaInAs device can easily be written as

$$V = \frac{k_B T}{e}\left[\ln\left(\frac{J_{sc_t} - J}{J_{o_t}} + 1\right) + \ln\left(\frac{J_{sc_b} - J}{J_{o_b}} + 1\right)\right], \quad (1)$$

where k_B is Boltzmann's constant, T is the absolute temperature and e is the electronic charge. J_{sc_i}, J_{o_i} (i = t, b) denote the photocurrent and dark current for the top (with the subscript t) and bottom one (with the subscript b), respectively, which can be further determined as follows.

$$J_{sc_t} = \sum_{\lambda} eI(\lambda)QE_t(\lambda)\Delta\lambda, \quad (2)$$

$$J_{sc_b} = \sum_{\lambda} eI(\lambda)\exp(-\alpha_t(\lambda)t_t)QE_b(\lambda)\Delta\lambda, \quad (3)$$

where $I(\lambda)$ is the incident spectrum density as a function of wavelength, $\alpha_t(\lambda)$ is the absorption coefficient of the top cell, and t_t is the top cell thickness. For the realistic QE_i, as mentioned above, we must consider the potential effect of several realistic parameters on QE, including the minority carrier's diffusion length, the absorption coefficient of materials, surface recombination velocity, etc. Furthermore, QE can be derived by solving the minority-carrier diffusion equation with boundary conditions in the p–n junction in Ref. [13].

In addition, the dark current density J_o[9] is also given by

$$J_o = q\frac{D_p}{L_p}\frac{n_i^2}{N_d}\frac{\frac{S_pL_p}{D_p}\cosh\frac{X}{L_p} + \sinh\frac{X}{L_p}}{\frac{S_pL_p}{D_p}\sinh\frac{X}{L_p} + \cosh\frac{X}{L_p}} + q\frac{D_n}{L_n}\frac{n_i^2}{N_a}\frac{\frac{S_nL_n}{D_n}\cosh\frac{H}{L_n} + \sinh\frac{H}{L_n}}{\frac{S_nL_n}{D_n}\sinh\frac{H}{L_n} + \cosh\frac{H}{L_n}}, \quad (4)$$

where n_i is the intrinsic carrier concentration of the material, as a function of E_g. S_n and S_p are the surface recombination velocities in the n- and p-type layers, N_a and N_d are the acceptor and donor concentrations, respectively. The quantities D_p, L_p, D_n, L_n are, respectively, the diffusion coefficient and diffusion length for the minority carriers in the emitter layer and base layer, which have the following relations:

$$D = \frac{k_B T\mu}{q}, \quad L = \sqrt{D\tau}, \quad \tau = \frac{1}{BN}, \quad (5)$$

where μ and τ are the mobility and minority carrier lifetime, respectively. B is the radiative recombination coefficient, and N is the majority carrier concentration. Specific material parameters assigned for each subcell can be found in previously published papers[9, 13].

The maximum-power point (J_{mp}, V_{mp}) can be derived by solving the equation:

$$\frac{d(JV)}{dJ} = 0. \quad (6)$$

The η can be obtained through the maximum-power divided by the total light power density. Therefore, we built a relationship between the η and the E_g of the top and bottom cells.

3. Results and discussions

Now we will show the results of our numerical calculations, and the optimal combination of E_g is first discussed. Figure 2 plots isoefficiency contours for the dual-junction system in the dependence of subcell E_g under AM1.5d at 300 suns, with the assumption of thickness for both subcells being infinite. In comparison to the lattice-matched $GaInP_2$/GaAs system, it is evidently seen that the η can be effectively enhanced by decreasing the E_g of both subcells by raising the indium content. For example, the specific η in our calculation can be enhanced from 35.48% (point E) for a well lattice-matched system to the highest one 44.6% (point D). Unfortunately, due to the induced large mismatch between subcells and substrate, this promising number might be unattainable for a realistic device because of considerable crystal defects, which usually act as effective recombination centers and thus cause degradation of device performance. Given that the mismatch between the cell active layers and substrate can be effectively relaxed by growing a proper buffer layer[2, 3, 14],the improvement of device performance would be experimentally available as indicated with the red line, where the lattice-matched relationship between subcells is held[15]. To see this point more clearly, we have extracted the corresponding efficiencies as a function of

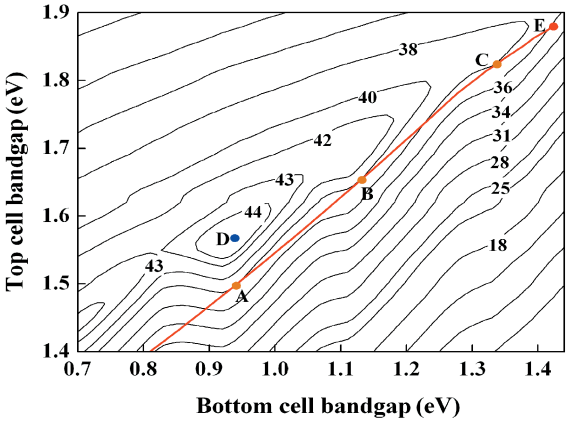

Fig. 2. (Color online) Contour plot of GaInP/GaInAs efficiencies under AM1.5d at 300 suns. The lattice-matched E_g combinations between GaInP top and GaInAs bottom cells are indicated by the thick line.

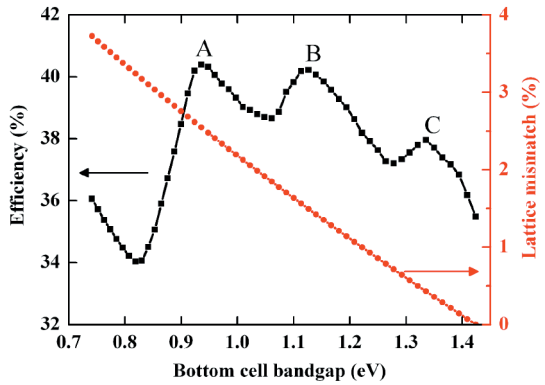

Fig. 3. (Color online) The η of the lattice-matched system versus the bottom cell E_g. The lattice mismatch for the bottom cell to the GaAs substrate is also indicated.

bottom cell E_g in Fig. 3. For the comparison, the misfit between the cells and substrate is also shown. Obviously, three extreme points are easily obtained as 40.39% for combination A (1.495 eV, 0.936 eV), 40.22% for B (1.65 eV, 1.127 eV) and 37.962% for C (1.83 eV, 1.335 eV). Although superior efficiency beyond 40% can be expected for combinations A and B, larger mismatch is also induced for these combinations, i.e., 2.5% for A and 1.5% for B. Realistic fabrication would be a great challenge under such a huge lattice mismatch. Moreover, combination C has an efficiency of 37.96%, which shows 2.5% improvement compared to the traditional $GaInP_2$/GaAs system. In addition, the lattice mismatch between cells and substrate is only 0.43%, an acceptable number in practice.

The calculations above are based on the assumption that both subcells are of infinite thickness. In order to predict more realistic efficiencies, one must go into the details of the specific device structure, including the design for the top and bottom cell thicknesses, which have been already controlled accurately in experiments by modern material growth technology such as metal organic vapor phase epitaxy (MOVPE). Obviously, the adjustment of thickness would reallocate the solar spectrum ab-

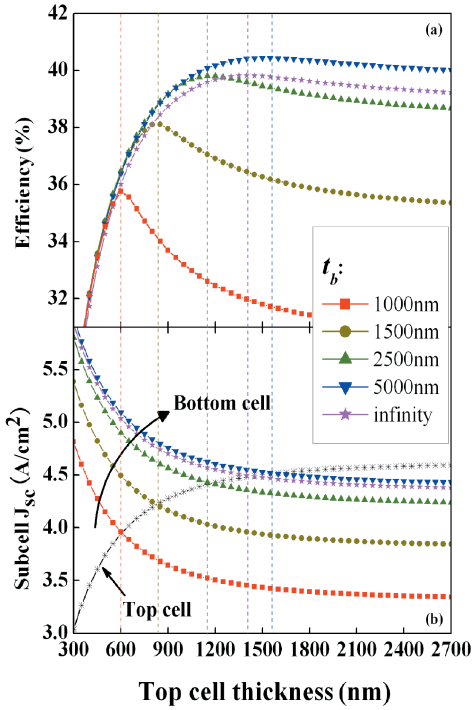

Fig. 4. (Color online) The J_{SC} of each subcell and the device's η as a function of t_t, within a range of different t_b, for an E_g combination (1.83 eV, 1.335 eV) dual-junction cell.

sorbed by subcells and thus has a significant impact on the performance of the PV cell. Therefore, in the following paragraph we mainly investigate the effect of each subcell's thickness on the performance of combination C and conduct further optimization of the device structure, which provides a guideline for the next step of fabricating this configuration.

Figure 4 shows the J_{sc} of each subcell and the corresponding η as a function of top cell thickness (t_t) for different bottom cell thicknesses (t_b) under AM1.5d at 300 suns. One can clearly see that every given t_b corresponds to a couple of curves of the subcell's J_{sc} and a curve of the PV cell's η. When t_t is lower than the optimum thickness, the top cell cannot absorb all the incident photons above its E_g, and a fraction of them is transmitted and absorbed in the bottom cell. Thus the current density of bottom cell (J_{sc_b}) is larger than that of the top cell (J_{sc_t}). Since the J_{sc} of a series-connected device is limited to the lesser of $J_{sc_t}$and J_{sc_b}, the top cell must be thickened until it reaches $J_{sc_t} = J_{sc_b}$, where maximum η is obtained, with a corresponding t_t considered as the optimum t_t.

On the other hand, it is seen in Fig. 4 that as t_b increases from 1000 to 5000 nm, the optimum t_t and peak η shift to the larger t_t side, which is mainly because there are more photons absorbed in an increasing-thickness bottom cell, leading to the increase of J_{sc_b} and corresponding η. However, when further thickening the bottom cell until it reaches infinity, there is a slight decrease in the optimum t_t and η as shown in Fig. 4. This shows that t_b indeed has an influence on device performance. But in some published papers[9, 12], the calculations were all based on the assumption that t_t was adjustable while t_b was infinitely thick. That coarse assumption, in some cases, results

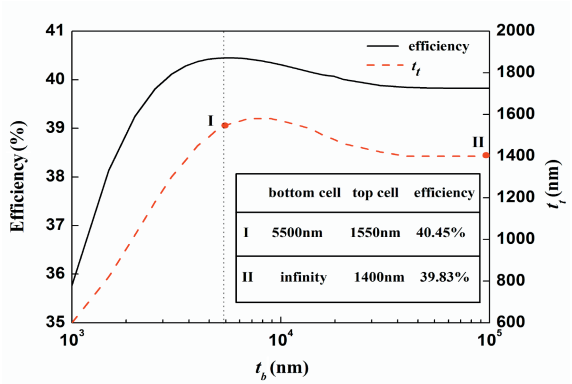

Fig. 5. (Color online) The optimum t_t and maximum η as a function of t_b, for an E_g combination (1.83 eV, 1.335 eV) PV cell.

in slightly lower theoretical η due to the misestimate of an optimum t_t. Therefore, for maximizing the device's η, t_b should be considered here and optimized based on the current match condition.

As we know, at a certain t_b, the optimum t_t and maximum η could be obtained at the current match point. According to this, Figure 5 illustrates the dependence of the optimum t_t and maximum η on the t_b. In a low-t_b region, the reason for the increase in the optimum t_t and corresponding maximum η with increasing t_b has been analyzed in the previous discussions. After exceeding a t_b of 5500 nm (point I), the maximum η starts to decline slowly and finally reaches a saturation value (point II). Similar behavior is also observed for the optimum t_t, the decrease in which is mainly attributed to the effect of minority carrier recombination on J_{sc}, which is just considered in our improved model while ignored in previous works[7−10]. Concretely speaking, if photo-generated carriers want to make a contribution to J_{sc}, they must be collected effectively by the p–n junction before recombining. With the increase of t_b, a fraction of the minority carriers are generated away from the junction-depletion region and the collection probability of them would drop significantly. Therefore, there is a higher probability of recombination before the minority carriers reach the depletion region and are swept apart by the electric field, and thus the corresponding J_{sc_b} decreases, leading to the decline in the optimum t_t determined by making $J_{sc_t} = J_{sc_b}$. While the bottom cell is thick enough to absorb all the photons above its bandgap, the optimum t_t would reach a saturation value as shown in Fig. 5.

4. Summary

In summary, the design and optimization of a GaInP/GaInAs dual-junction cell have been conducted by integrating a set of practical material parameters with a realistic QE, which would be more in line with the real situation. Our numerical calculations showed the dependence of theoretical η on the E_g of subcells. Compared to the well-developed $GaInP_2$/GaAs system, an improvement of η has been observed for a novel metamorphic E_g combination (1.83 eV, 1.335 eV), with an acceptable misfit to the GaAs substrate. For the suggested structure, the optimum thickness of each subcell has been calculated, which results in a higher theoretical η up to 40.45% (300 suns, AM1.5d) and becomes a practical guideline for the subsequent fabrication of this tandem PV cell.

References

[1] Cotal H, Fetzer C, Boisvert J, et al. III–V multijunction solar cells for concentrating photovoltaics. Energy & Environmental Science, 2009, 2(2): 174
[2] King R R, Law D C, Edmondson K M, et al. 40% efficient metamorphic GaInP/GaInAs/Ge multijunction solar cells. Appl Phys Lett, 2007, 90: 183516
[3] Geisz J F, Friedman D J, Ward J S, et al. 40.8% efficient inverted triple-junction solar cell with two independently metamorphic junctions. Appl Phys Lett, 2008, 93: 123505
[4] Guter W, Schone J, Philips P, et al. Current-matched triple-junction solar cell reaching 41.1% conversion efficiency under concentrated sunlight. Appl Phys Lett, 2009, 94: 223504
[5] Yamaguchi M. Multi-junction solar cells and novel structures for solar cell applications. Physica E, 2002, 14(1): 84
[6] Garcia I, Rey-Stolle I, Galiana B, et al. A 32.6% efficient lattice-matched dual-junction solar cell working at 1000 suns. Appl Phys Lett, 2009, 94: 053509
[7] King R R, Sherif R A, Law D C, et al. New horizons in III–V multijunction terrestrial concentrator cell research. Proc 4th Int Conf on PV Solar Energy (Dresden, Germany), 2005: 124
[8] Gergo L, Bett A W. EtaOpt—a program for calculating limiting efficiency and optimum bandgap structure for multi-bandgap solar cells and TPV cells. 17th European PV Solar Energy Conf, 2001: paper VA1.25
[9] Kurtz S R, Faine P, Olson J M. Modeling of two-junction, series-connected tandem solar cells using top-cell thickness as an adjustable parameter. J Appl Phys, 1990, 68: 1890
[10] Dimroth F, Beckert R, Meusel M, et al. Metamorphic GaInP/GaInAs tandem solar cells for space and for terrestrial concentrator applications at $C > 1000$ suns. Progress in Photovoltaics: Research and Applications, 2001, 9: 165
[11] http://rredc.nrel.gov/solar/spectra/am1.5/
[12] Zhang Xiaobin, Wang Xiaoliang, Xiao Hongling, et al. Theoretical design and performance of InGaN two-junction solar cells. J Phys D: Appl Phys, 2008, 41: 245104
[13] Luque A, Hegedus S. Handbook of photovoltaic science and engineering. New York: John Wiley & Sons Ltd, 2003: 359
[14] Bett A W, Baur C, Dimroth F, et al. Metamorphic GaInP–GaInAs layers for photovoltaic applications. Materials for Photovoltaics Symposium, 2005, 836: 223
[15] Kasap S, Capper P. Handbook of electronic and photonic materials: part D materials for optoelectronics and photonics: chap 31. Springer, 2007: 735